Preparation and Performance of Cu-Cr Contact Materials for Vacuum Switches with Low Contact Pressure

Yanli Chang, Wei Zheng, Zhiming Zhou, Yuxiang Zhai & Yaping Wang

Journal of Electronic Materials

ISSN 0361-5235

Journal of Elec Materi
DOI 10.1007/s11664-016-4782-0

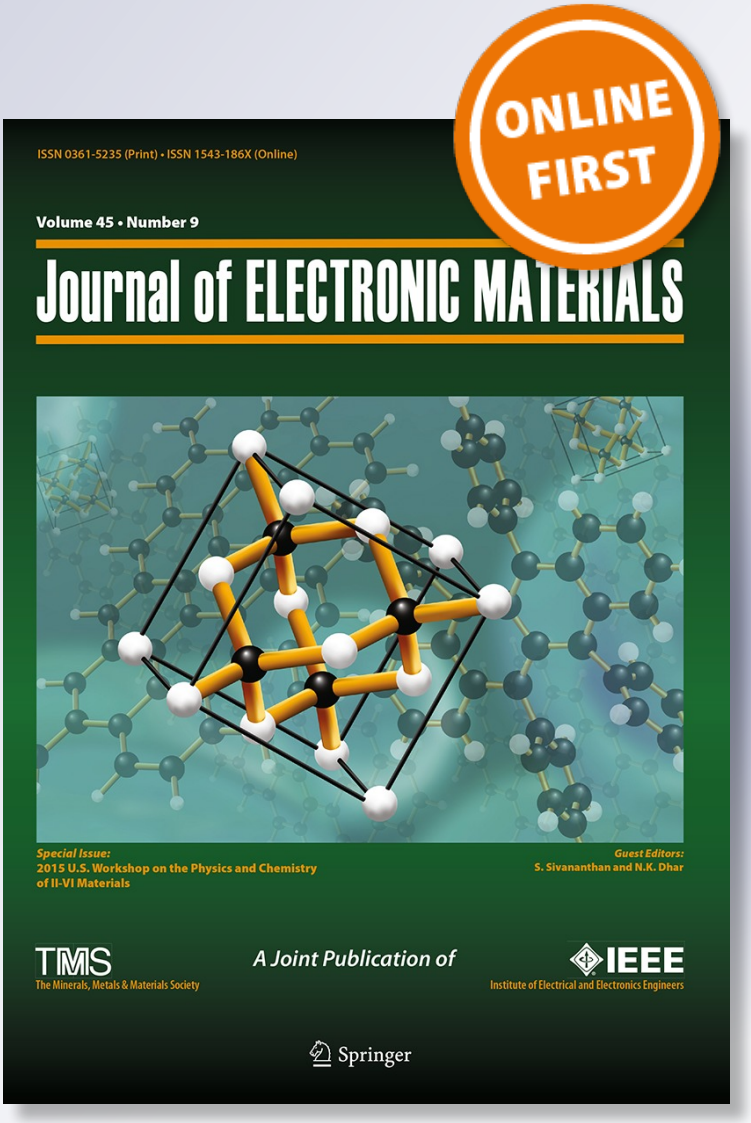

Springer

Journal of ELECTRONIC MATERIALS
DOI: 10.1007/s11664-016-4782-0

Preparation and Performance of Cu-Cr Contact Materials for Vacuum Switches with Low Contact Pressure

YANLI CHANG,[1,4] WEI ZHENG,[1] ZHIMING ZHOU,[2] YUXIANG ZHAI,[1] and YAPING WANG[1,3,5]

1.—MOE Key Laboratory for Nonequilibrium Synthesis and Modulation of Condensed Matter, School of Science, Xi'an Jiaotong University, Xi'an 710049, People's Republic of China. 2.—School of Material Science and Engineering, Chongqing University of Technology, Chongqing 400054, People's Republic of China. 3.—State Key Laboratory for Mechanical Behavior of Materials, Xi'an Jiaotong University, No. 28, Xianning West Road, Xi'an, Shaanxi 710049, People's Republic of China. 4.—e-mail:1063058286@qq.com. 5.—e-mail: ypwang@mail.xjtu.edu.cn

Insufficient anti-welding properties limit the application of Cu-Cr contact material in vacuum switches with low contact pressure. The CuCr-W-C alloys that are prepared are for decreasing welding tendencies and keeping the voltage withstand by addition of W and C elements. It is found that the average welding force of CuCr-W-C alloys is reduced more than 50% compared with that of the Cu_{50} Cr_{50} alloy. Especially for $CuCrW_{3.0}C_{0.3}$ and $CuCrW_{1.0}C_{0.5}$, the welding forces reduce to only 10% of $Cu_{50}Cr_{50}$. Arc erosion areas of CuCr-W-C alloys are enlarged by five times more than that of the $Cu_{50}Cr_{50}$ alloy in the same arcing conditions. The results of type tests were qualified. The results suggested that the $CuCrW_{2.0}C_{1.0}$ alloy could be used in vacuum switches with low contact pressure to replace the W-Cu type contacts.

Key words: CuCr-W-C, vacuum switch, low contact pressure, anti-welding

INTRODUCTION

Low contact pressure is expected for vacuum switches because of the potential advantage in miniaturization, high operating frequency, and especially for the low voltage utilization with the mechanical structure operated by low power.[1] The vacuum switches with lower contact pressure require contact materials having enough welding resistance while not losing breaking capacity and voltage withstand.

Due to their high breaking capacity and high voltage withstand, Cu-Cr alloys are widely utilized in vacuum interrupters.[2–7] However, their high welding inclination during operation requires high operation power of the mechanical structure and limits their utilization in switches with low contact pressure. So, the vacuum contactors and load switches, which usually are driven by the low power structures, have to adopt Cu-W or Cu-WC type contacts with weak breaking capacity.[8] It was reported that the additives with low melting points can increase the welding resistance of Cu-Cr contacts, but meanwhile, decrease the dielectric strength and service life of the vacuum switches.[9]

The welding resistance mainly depends on tensile strength and fracture energy of the welding zone of the contact materials. It was found that small amounts of C (0.2–1.8%) can reduce oxygen content and generate brittle chromium carbides $Cr_{23}C_6$.[10,11] Chromium carbides $Cr_{23}C_6$ can decrease welding strength, but meanwhile, breakdown strength was reduced.[12] W can significantly refine grain size of the Cr phase and, thus, improve breakdown strength of the alloy.[13]

In this work, the CuCr-W-C alloys are prepared in order to provide a kind of contact with a low welding tendency and high voltage withstand as well as high breaking capacity. The effects of tungsten and carbon on the microstructure, arc erosion, separating force, and fracture mode were investigated. A vacuum arc observation platform was set up to study separating force.

(Received August 20, 2015; accepted June 30, 2016)

Published online: 27 July 2016

EXPERIMENT

CuCr-W-C alloys were manufactured by the vacuum infiltration method. The manufacturing technology includes mixing raw Cr powder, W powder, and C powder according to the proportion in Table I, pressing, sintering to a porous matrix, and then infiltrating with copper in a vacuum. The detailed preparation method was described in Refs. 14 and15

The chemical composition, conductivity, and hardness of CuCr-W-C alloys were measured. A HVS-502 machine was used to determine the Vickers hardness of CuCr-W-C alloys. Electrical conductivity was measured by an eddy-current conductivity meter. The microstructure and fracture surface after the tensile experiment were observed by a JEOL JSM-7000F type scanning electron microscope (SEM). The distribution of Cr, W, and C in the CuCr-W-C alloys were determined by an energy dispersion spectrum (EDS) attached to the SEM.

Arcing erosion was carried out in a vacuum arc observation platform, which was indigenously manufactured (as is shown in Fig. 1). Discharge waveforms were recorded by a Tektronix DPO4034 type digital memory oscillograph. In order to simulate the operating condition of a vacuum interrupter, a welding test was carried out with the discharge of a capacitor in the vacuum furnace at a pressure of

Table I. Proportion of Cr powder, W powder, and C powder

Number of sample	Alloy	Proportion of Cr powder, W powder, and C powder		
		Cr/wt.%	W/wt.%	C/wt.%
1#	$Cu_{50}Cr_{50}$	100.0	0.0	0.0
2#	$CuCrW_{1.0}$	98.0	2.0	0.0
3#	$CuCrW_{3.0}$	94.5	5.5	0.0
4#	$CuCrW_{1.0}C_{0.3}$	97.5	2.0	0.5
5#	$CuCrW_{3.0}C_{0.3}$	94.0	5.5	0.5
6#	$CuCrW_{1.0}C_{0.5}$	97.0	2.0	1.0
7#	$CuCrW_{3.0}C_{0.5}$	93.5	5.5	1.0
8#	$CuCrW_{3.0}C_{0.8}$	93.0	5.5	1.5
9#	$CuCrW_{2.0}C_{1.0}$	94.5	3.5	2.0
10#	$CuCrW_{4.0}C_{1.0}$	90.5	7.5	2.0
11#	$CuCrW_{5.7}C_{1.0}$	88.0	10.0	2.0

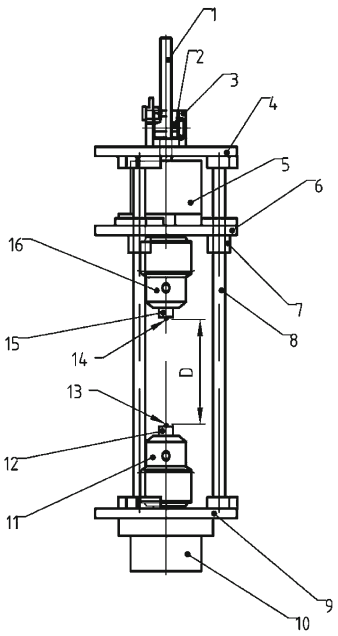

1-screw, 2-positioning nut, 3-releasing mechanism, 4-highest quotations, 5- clump weight, 6-support for moving contactor, 7-linear bearings on precision round-ways, 8-Precision linear rail, 9-chasis, 10-pedestal, 11- fixed contactor clamp, 12-fixed contactor sample, 13-contact surface of fixed contact, 14-contact surface of moving contactor, 15-moving contactor sample, 16-moving contactor clamp.

Fig. 1. structure diagram of vacuum arc observation platform. 1-screw, 2-positioning nut, 3-releasing mechanism, 4-highest quotations, 5-clump weight, 6-support for moving contactor, 7-linear bearings on precision round-ways, 8-Precision linear rail, 9-chasis, 10-pedestal, 11-fixed contactor clamp, 12-fixed contactor sample, 13-contact surface of fixed contact, 14-contact surface of moving contactor, 15-moving contactor sample, and 16-moving contactor clamp.

2×10^{-3} Pa. The capacitance of the capacitor was 360 uF. The capacitor was charged with a high voltage generator. The voltage was a constant 4 kV.

A Phantom V9.0 high-speed camera was used to shoot movements of arc spots and record arc spot distribution. The separating force was tested in a WDW-100C microcomputer control electron universal testing machine.

The type test was implemented in the China National Center for Quality Supervision and Test of Electrical Apparatus Products. Flat CuCr-W-C contacts were installed in a TJ—7.2/450 vacuum arcing chamber. An external magnetic field was applied outside the vacuum chamber to increase the breaking capacity. The loop resistance, temperature-rise, and short-time power frequency withstand were tested.

Table II. Parameters of CuCr-W-C alloys

Material	Conductivity/ MS m^{-1}	Hardness/ HV
$Cu_{50}Cr_{50}$	14.3	83.4
$CuCrW_{1.0}$	15.7	90.8
$CuCrW_{3.0}$	15.0	96.4
$CuCrW_{1.0}C_{0.3}$	13.0	98.0
$CuCrW_{3.0}C_{0.3}$	15.5	118.3
$CuCrW_{1.0}C_{0.5}$	13.9	140.7
$CuCrW_{3.0}C_{0.5}$	16.7	106.7
$CuCrW_{3.0}C_{0.8}$	16.8	112.0
$CuCrW_{2.0}C_{1.0}$	15.8	124.8
$CuCrW_{4.0}C_{1.0}$	16.3	101.3
$CuCrW_{5.0}C_{1.0}$	13.6	138.8

RESULTS AND DISCUSSION

Electrical conductivity and hardness of CuCr-W-C alloys are shown in Table II. It can be seen that the addition of W and C elements can increase the hardness from 8.9% to 68.7% as compared with that of CuCr alloys without additives. Little effect was found on the electrical conductivity of Cu-Cr alloys by the addition of W and C elements.

The microstructures of CuCr-W-C alloys are shown in Fig. 2. The gray area is the Cr phase, the light area is the Cu matrix and the white spot is the W particle. It can be seen that the size of the Cr

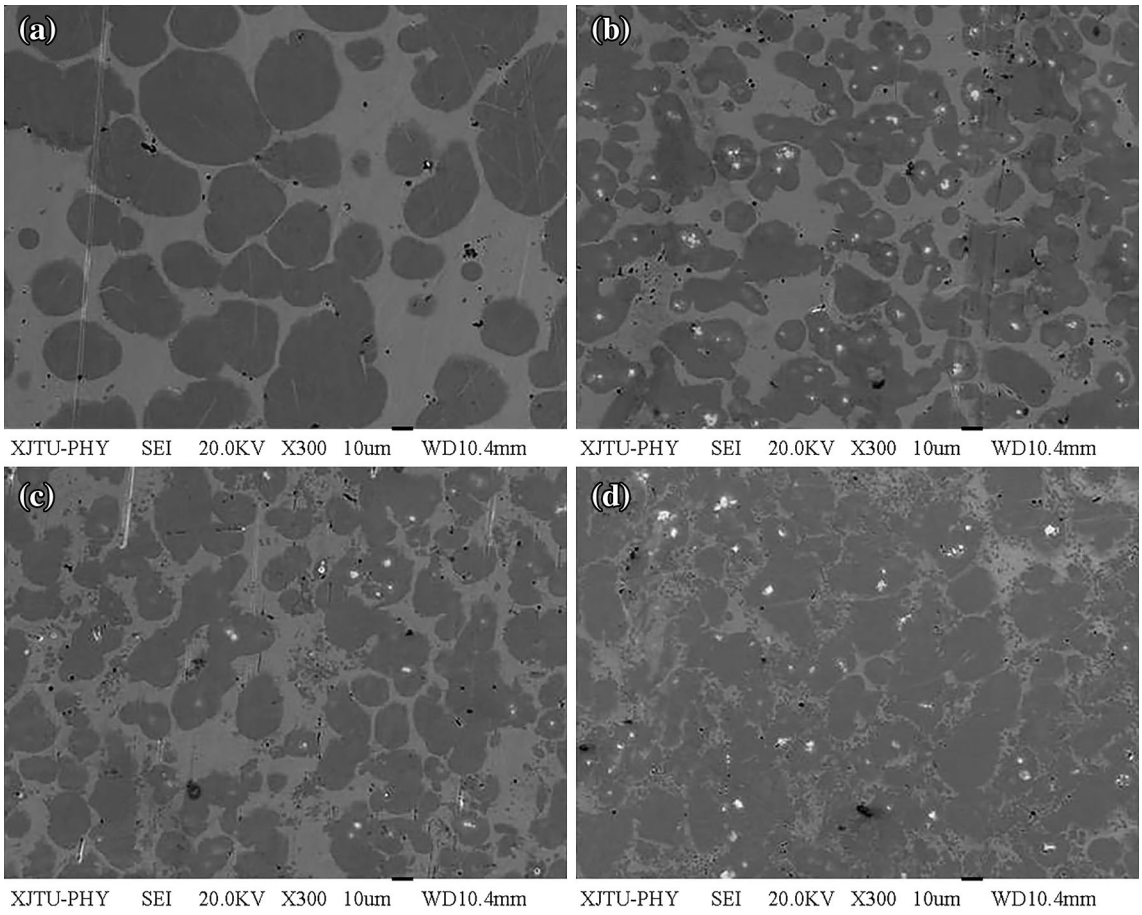

Fig. 2. Microstructure of CuCr-W-C contact material (a) $Cu_{50}Cr_{50}$ (b) $CuCrW_{3.0}C_{0.3}$ (c) $CuCrW_{1.0}C_{0.5}$ (d) $CuCrW_{2.0}C_{1.0}$.

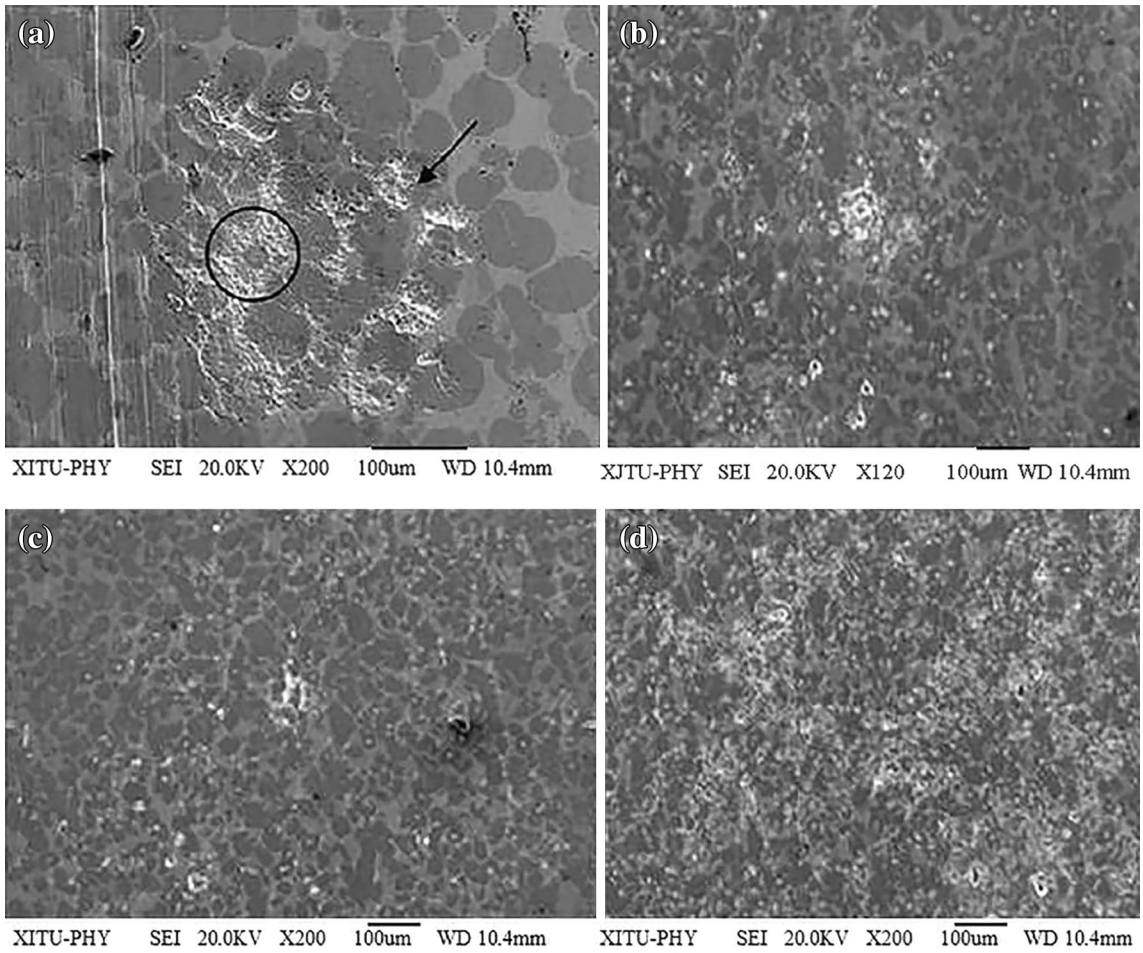

Fig. 3. Ablation morphology of the cathode surface after first breakdown. (a) $Cu_{50}Cr_{50}$ (b) $CuCrW_{3.0}C_{0.3}$ (c) $CuCrW_{1.0}C_{0.5}$ (d) $CuCrW_{2.0}C_{1.0}$.

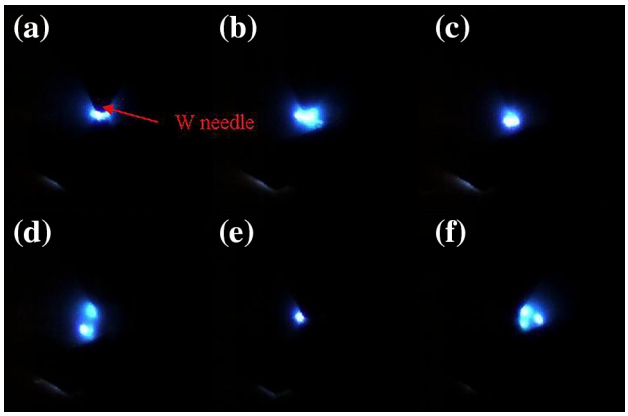

Fig. 4. The arc spots fission during arcing of $CuCrW_{2.0}C_{1.0}$ contact (a)1st card (b) 9th card (c) 13th card (d)17th card (e) 23rd card (f) 29th card.

phase is reduced by adding W and C. When the content of W is more than 1.0%, the average size of the Cr particles is around 20 μm. From Fig. 2a–d, the Cu-Cr interface becomes more and more fuzzy and flocculent. In Fig. 2d, the Cr phase margin appears dissolved and melted. This kind of microstructure is helpful to reduce the welding area of the copper phase and improve the anti-welding property.

From Fig. 3, it can be seen that firstly breakdown occurs on a grain boundary. Arc erosion areas of CuCr-W-C alloys were enlarged by 5five times, compared with that of $Cu_{50}Cr_{50}$ alloy in the same arcing condition. Especially for $CuCrW_{2.0}C_{1.0}$, it was almost enlarged to 12 times. For the $CuCrW_{2.0}C_{1.0}$ alloy, the arcing zone was mainly located on Cr particles with the size of 1–3 μm and a neighboring Cu matrix. The arcing zone was barely located on the Cr particle with a size more than 40 μm. It is inconsistent with a traditional conclusion that firstly breakdown occurs on large-size Cr particles because of their low thermal conductivity.[16,17]

Figure 4 shows the process of arc spotting by high-speed photography. It was found that arc duration was 2 ms. Arc spots are big and bright at first and then split into two spots around 664 μs.

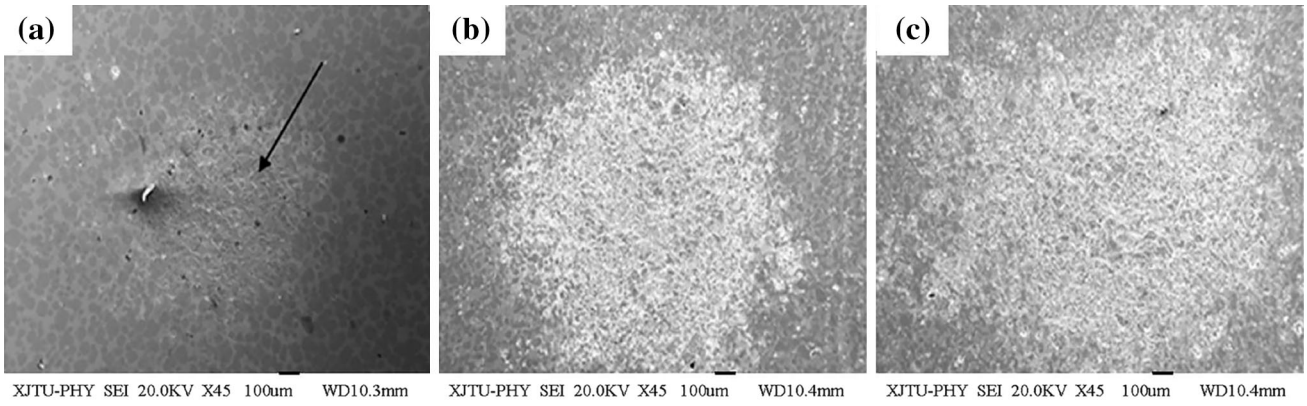

Fig. 5. Morphology of the cathode surface ablation after breakdown 100 times (a) $Cu_{50}Cr_{50}$ (b) $CuCrW_{1.0}C_{0.5}$ (c) $CuCrW_{2.0}C_{1.0}$.

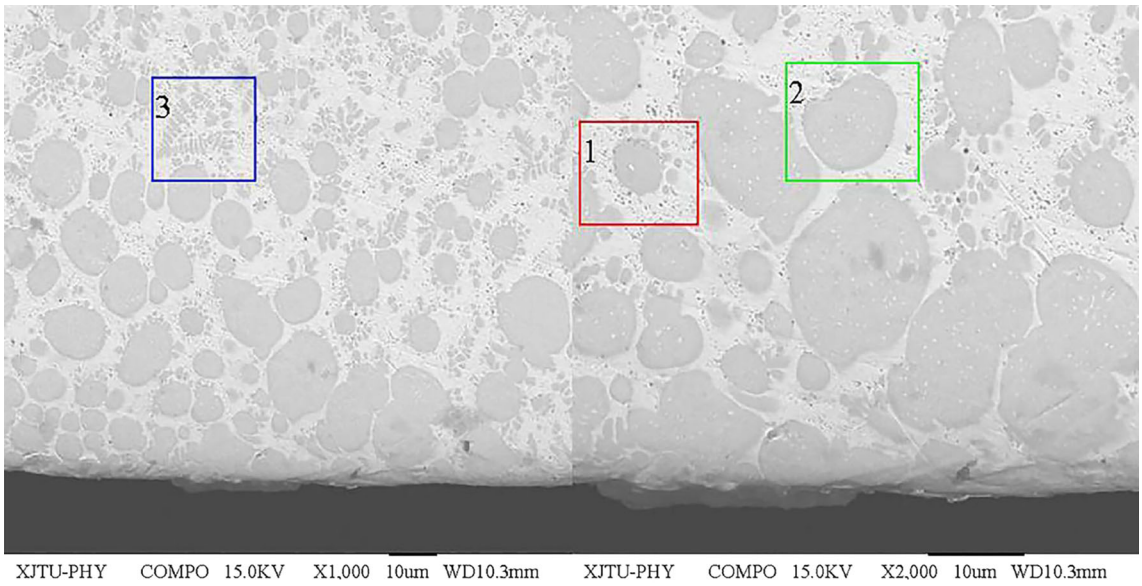

Fig. 6. The cross-section microstructure of CuCr-W-C alloys after breaking of 3000 A current in the vacuum contactor.

After splitting into three spots in 1162 μs (29th card), spots extinguish.

Scatter and fission of arc spots can significantly reduce the melting degree of the electrode surface, which is a benefit from improving ablation resistance, current breaking capacity, and voltage withstanding of the electrode materials.[18,19]

From Fig. 5a, it can be seen that the arcing spots of $Cu_{50}Cr_{50}$ alloy are centralized, and the subsequent corrosion pits are deep (black arrow). For CuCr-W-C alloys, breakdown exhibits diffusional features in which the arc moves to the larger contact surface. Especially for $CuCrW_{1.0}$ $C_{0.5}$ and $CuCrW_{2.0}$ $C_{1.0}$ alloys, there are barely deep pits.

From Fig. 6, it can be seen that at the surface layer of the alloys occurs melting and recrystallization. During crystallization, Cr forms three different microstructures: liquid phase separation microstructure (zone 1), solidification microstructure by the nucleus of W particles (zone 2), and Cr dendritic microstructure (zone 3). It was shown that additives increased the solidification rate by the nucleus of W particles, which is a benefit for the voltage withstand and interruption capability.

Figure 7 shows the content effect of W and C additives on separating force. From Fig. 7, it can be seen that the welding resistance of CuCr-W-C alloys obviously improves . The average separating force of CuCr-W-C alloys reduces more than 50% compared with that of $Cu_{50}Cr_{50}$. Especially for $CuCrW_{3.0}C_{0.3}$ and $CuCrW_{1.0}C_{0.5}$ alloys, the average separating forces reduce to only 10% of $Cu_{50}Cr_{50}$.

The criterion equation of welding resistance is k_{ω},[20–22]

$$k_{\omega} = \frac{\theta_m \sqrt{c_p \rho_m \lambda}}{\rho_d} \cdot \frac{a_0}{\pi \sigma}, \tag{1}$$

where θ_m is melting point, c_p is specific heat, ρ_m is density, λ is conductivity, ρ_d is resistivity, and σ is welding layer strength. The bigger the k_{ω},

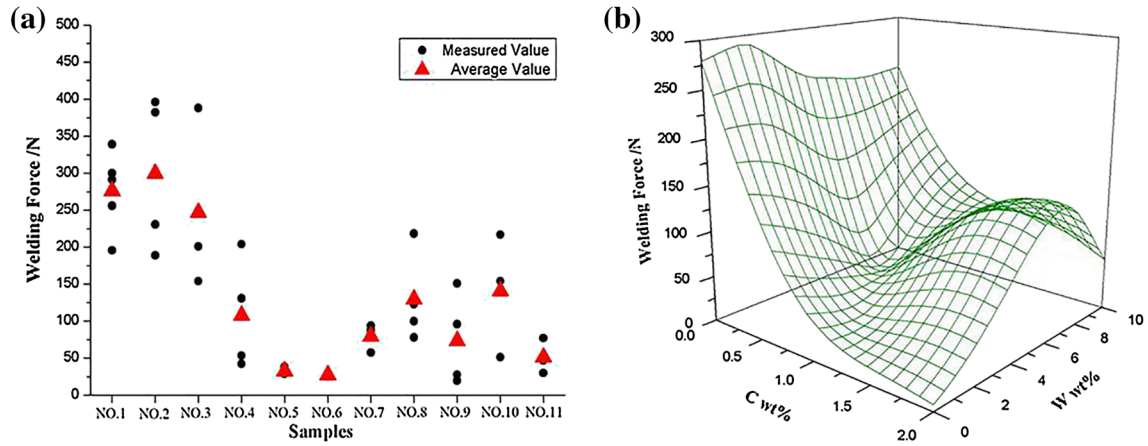

Fig. 7. The content effect of W and C additives on separating force (a) Welding force of samples (b) Welding force and content of W and C curve.

Table III. The project and results of the type test

Test item	Test condition	Result
Loop resistance	Main loop resistance ≤180 $\mu\Omega$	Good
Temperature-rise	450 A	Good
Short-time power frequency withstand voltage	Earth, alternate and port: 25 kV, 1 min	Good
Lightning impulse withstand test	Earth, alternate and port: 40 kV peak	Good
Make-break ability (AC4)	3.6 kV make current: 4.5 kA 100 times	Good
	3.6 kV maximal break current: 3.6 kA 25 times	Good
	3.6 kV minimal break current: 90 A 25 times	Good
Over current withstand test	imposed current: 6750 A 1 s	Good
Short-time withstand current and peak withstand current	Main loop: 2 s 4.5 kA peak value: 11.25 kA	Good
Short-time current make—break test	3.6 kV 8.0 kA 3 times	Good
Extreme short-circuit current break test	3.6 kV 13 kA 3 times	Good

the better the welding resistance. Also, a_0 is the radius of the contact spot,

$$a_0 = \sqrt{\frac{F_c}{\pi H_c} + \left(\frac{3}{2}\cdot\frac{F_c R}{E}\right)^{2/3}}, \qquad (2)$$

where F_c is force, H_c is hardness, R is radius of contact, and E is the Elastic Modulus.

From the equations, it can be seen that welding force will decline with increase of hardness. The addition of W and C elements can significantly increase the hardness of CuCr-W-C alloys (Table II), decrease welding force, and then improve welding resistance.

Figure 8 shows the fracture morphology of CuCr-W-C alloys, with separating forces that are relatively low (28–74 N). From Fig. 8, it can be seen that the microstructure of the welding layer have many similar characteristics, which were listed as follows: (1) grain size is refined and welding layer is deep and small, (2) welding layer is a mainly brittle and porous microstructure, and (3) the fracture mechanism is mainly a brittle fracture.

The separating force mainly depends on welding tendency and welding layer strength. The mechanism of carbon on reducing the welding force lies in generating brittle chromium carbides $Cr_{23}C_6$ and residual free C fall off and formation of carbon holes during stretching, which can remarkably promote crack initiating and propagating. At the nucleus of the solidification zone, W particles can refine grain, which is a benefit to the dielectric strength and hardness. On the other hand, the hard particles will decrease the welding layer's fracture energy by second phase strengthening.

Welding force is not only related to microstructure and composition of material but also affected by surface properties of contact, contact spring, contact status, and so on.[23,24]

Table III summarizes type test project and test results of $CuCrW_{2.0}C_{0.5}$ contacts. From Table III, it can be seen that the results of the type test were qualified. The results suggested that $CuCrW_{2.0}C_{1.0}$

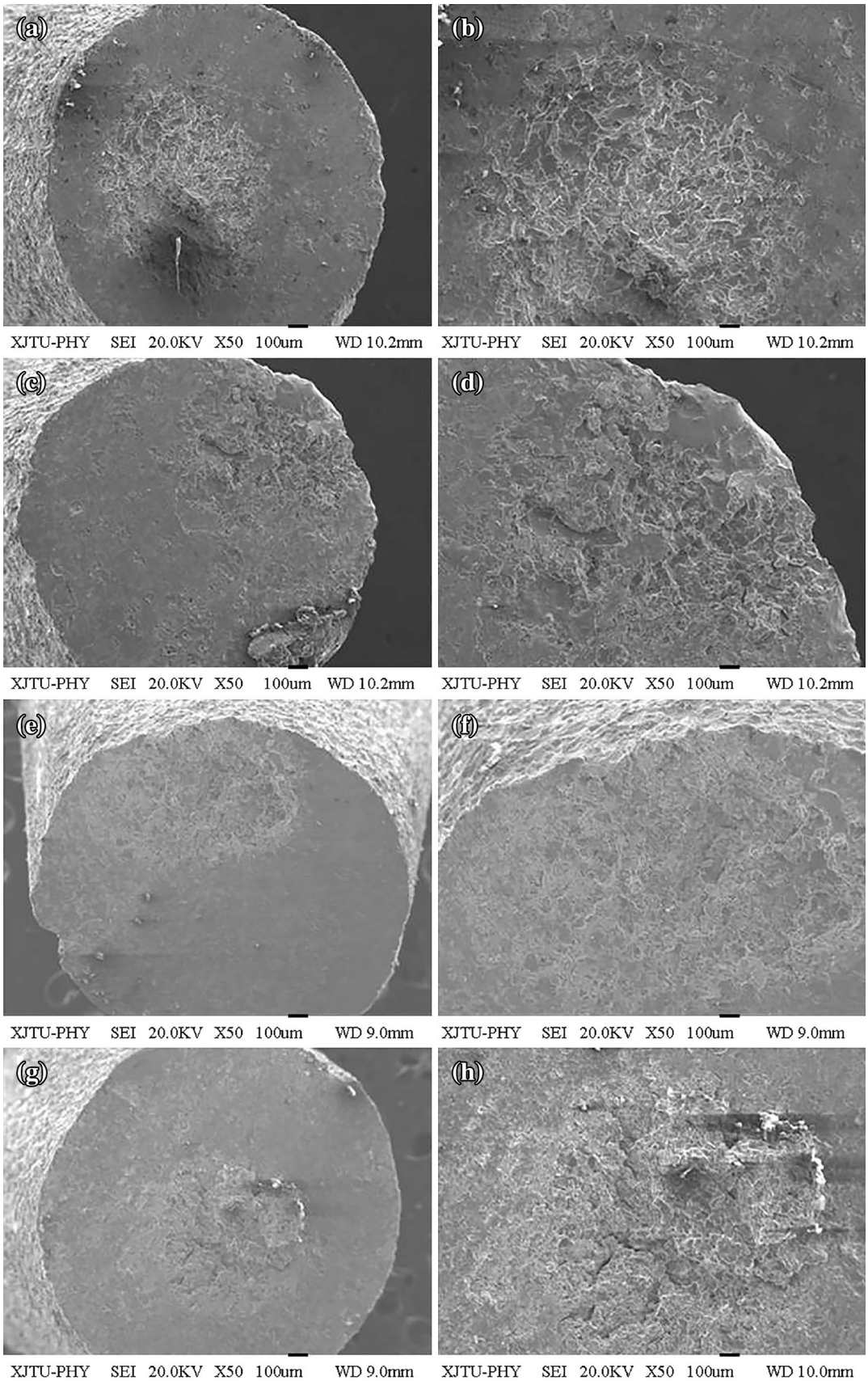

Fig. 8. The fracture morphology of the welding surface (a) $CuCrW_{3.0}C_{0.3}$, (c) $CuCrW_{1.0}C_{0.5}$, (e) $CuCrW_{2.0}C_{1.0}$, (g) $CuCrW_{5.0}C_{1.0}$. (b), (d), (f), and (h) are details with enlarged scale of (a), (c), (e), and (g).

alloy could be used in the vacuum switches with low contact pressure to replace the W-Cu type contacts.

CONCLUSIONS

The effect of W and C elements on welding resistance and arcing behavior were studied. Results show that addition of W and C elements can significantly increase the hardness and have little effect on the electrical conductivity of Cu-Cr alloys. The arc erosion area of CuCr-W-C alloys enlarged by five times. The average separating force of CuCr-W-C alloys is reduced by more than 50% compared with that of the $Cu_{50}Cr_{50}$ alloy. Especially, for the $CuCrW_{3.0}C_{0.3}$ and $CuCrW_{1.0}C_{0.5}$ alloys, the separating forces reduce to only 10% of that of $Cu_{50}Cr_{50}$. The mechanism of additives on reducing the separating force is thought to be from the brittle chromium carbides film and increasing the solidification rate by the nucleus of W particles, which is also of benefit for the voltage withstand and interruption capability. The type test of the vacuum switches proved the practicability by the CuCr-W-C alloy. It is concluded that the CuCr-W-C alloys are suitable to be used in the vacuum switches with low contact pressure to replace the W-Cu type contacts for their lower welding tendency while maintaining the voltage withstand and interrupting capability.

ACKNOWLEDGEMENTS

Thanks are given for the financial support of the National Science Foundation of China (51171146 and 51101177) and the Program for Key Science and Technology Innovative Research Team of Shaanxi Province (No. 2013KCT-05).

REFERENCES

1. P.G. Slade, *The Vacuum Interrupter: Theory, Design, and Application* (London: CRC Press Inc, 2007).
2. E. Walczuk, *Proceedings of the Thirty-Eighth IEEE Holm Conference on Electrical Contacts* (1992), pp. 1–16.
3. Z.B. Li, L.C. Chen, and J.Y. Zou, *Proceedings of the Forty-First IEEE Holm Conference on Electrical Contacts* (1995), pp. 346–349.
4. B.G. Qian, H.R. Geng, and Z.Q. Guo, *J. Rare Earths* 23, 378 (2005).
5. P.G. Slade, ed. *Electrical Contacts* (Marcel Dekker Inc., New York, 1999).
6. D. Bing-jun, W. Ya-ping, and Y. Zhi-mao, *IEEE Trans. DEI* 6, 913 (1999).
7. W. Yaping, Y. Zhimao, and D. Bing-jun, *IEEE Trans. DEI* 5, 245 (1998).
8. Z. Wei, W. Yaping, and W. Yongsheng, *High Vol. Appar.* 46, 69 (2010).
9. K. Ozawa, in *Proc International Conf on Electrical Contacts* (1986), pp. 823–830.
10. B.J. Ding, H.Q. Li, and X.T. Wang, *IEEE Trans. Compon. Hybrids Manuf. Technol.* 14, 386 (1991).
11. Z.M. Yang, S.P. Wei, and C.F. Qiu, *Electrical Contacts Proceedings of the Thirty-Eighth IEEE Holm Conference on Electrical Contacts* (1992), pp. 91–94.
12. M. Rong, *Electrical Contact Principle* (Bei Jing: China Machine Press, 2004).
13. J. Wang, C.Y. Zhang, and H. Zhang, *Trans. Nonferrous Metals Soc. China* 11, 226 (2001).
14. Z. Zhi-ming, W. Ya-ping, and Gao Jian-rong, *Mater. Sci. Eng., A* 398, 318 (2005).
15. W. Ya-ping, Z. Cheng-yu, and Z. Hui, *J. Phys. D Appl. Phys.* 36, 2649 (2003).
16. B.J. Ding, Z.M. Yang, and X.T. Wang, *IEEE Trans. Compon. Packag. Manuf. Technol. Part A:* 19, 76 (1996).
17. T. Seki, Y. Yamamoto, and T. Okutomi, *Proc 17th International Conf on Electrical Contact* (1994), pp. 879–886.
18. J. Halbritter, *IEEE Trans. Electron. Insul.* 20, 671 (1985).
19. Y.P. Wang and B.J. Ding, *IEEE Trans. Compon. Packag. Technol.* 22, 467 (1999).
20. L. Zhenbiao, Z. Guansheng, and Q. Qingsheng, *Proc. CSEE* 14, 34 (1994).
21. A.S. Budiman, K.R. Narayanan, N. Li, J. Wang, N. Tamura, M. Kunz, and A. Misra, *Mater. Sci. Eng. A* 635, 6 (2015).
22. A.S. Budiman, N. Li, Q. Wei, J.K. Baldwin, J. Xiong, H. Luo, D. Trugman, Q.X. Jia, N. Tamura, M. Kunz, K. Chen, and A. Misra, *Thin Solid Films* 519, 4137 (2011).
23. J.T. Wood, A.J. Griffin, J.D. Embury, R. Zhou, M. Nastasis, and M. Veront, *J. Mech. Phys. Solids* 44, 737 (1996).
24. A.S. Budiman, C.S. Hau-Riege, W.C. Baek, C. Lor, A. Huang, H.S. Kim, G. Neubauer, J. Pak, P.R. Besser, and W.D. Nix, *J. Electron. Mater.* 39, 2483 (2010).